



1 **Biogeochemical constraints on the origin of methane in an alluvial aquifer: evidence**
2 **for the upward migration of methane from a coal seam.**

3

4 Charlotte P. Iverach^{1,2,*}, Sabrina Beckmann³, Dioni I. Cendón^{1,2}, Mike Manefield³, Bryce
5 F.J. Kelly¹

6

7 ¹Connected Waters Initiative Research Centre, UNSW Australia, UNSW Sydney, NSW,
8 2052, Australia.

9 ²Australian Nuclear Science and Technology Organisation, New Illawarra Rd, Lucas
10 Heights, NSW, 2234, Australia.

11 ³School of Biotechnology and Biomolecular Sciences, UNSW Australia, UNSW Sydney,
12 NSW, 2052, Australia.

13

14

15

16

17

18

19

20

21

22

23

24



25 **Geochemical and microbiological indicators of methane (CH₄) production, oxidation**
26 **and migration processes in groundwater are important to understand when**
27 **attributing sources of gas. The processes controlling the natural occurrence of CH₄**
28 **in groundwater must be understood, especially when considering the potential**
29 **impacts of the global expansion of coal seam gas production on groundwater quality**
30 **and quantity. We use geochemical and microbiological data, along with**
31 **measurements of CH₄ isotopic composition ($\delta^{13}\text{C-CH}_4$), to determine the processes**
32 **acting upon CH₄ in a freshwater alluvial aquifer that directly overlies coal measures**
33 **targeted for coal seam gas production in Australia. Microbial and geochemical data**
34 **indicate that there is biogenic CH₄ in the aquifer, but no methanogenic microbial**
35 **activity. In addition, microbial community analysis showed that aerobic oxidation of**
36 **CH₄ is occurring. The combination of microbiological and geochemical indicators**
37 **suggests that the most likely source of CH₄, where it was present in the freshwater**
38 **aquifer, is the upward migration of CH₄ from the underlying coal measures.**

39

40 **Keywords:** Methane migration, groundwater, biogeochemistry, methanogenesis,
41 methanotrophy, coal seam gas, aquifer connectivity

42

43 **1 Introduction**

44 Interest in methane (CH₄) production and degradation processes in groundwater is driven
45 by the global expansion of unconventional gas production. There is concern regarding
46 potential impacts of gas and fluid movement, as well as depressurisation, on groundwater
47 quality and quantity in adjacent aquifers used to support other industries (Atkins et al.,
48 2015; Heilweil et al., 2015; Iverach et al., 2015; Moritz et al., 2015; Zhang et al., 2016).



49 In groundwater, CH₄ can originate from numerous sources (Barker and Fritz, 1981).
50 The two main sources of CH₄ in shallow groundwater are biological production
51 (biogenic) and upward migration of CH₄ from deeper geological formations (thermogenic
52 to mixed thermo-biogenic to biogenic) (Barker and Fritz, 1981; Whiticar, 1999). This
53 upward migration is via natural pathways such as geological faults and fracture networks
54 (Ward and Kelly, 2007), however it can also be induced via poorly installed wells and
55 faulty well casings (Barker and Fritz, 1981; Fontenot et al., 2013). The main focus of the
56 debate about the occurrence of CH₄ in groundwater is whether it is naturally occurring or
57 has been introduced by human activities. This research tests the hypothesis that a
58 combination of geochemical indicators and microbiological data can inform production,
59 degradation and migration processes of CH₄ in the Condamine River Alluvial Aquifer
60 (CRAA) in Australia. This freshwater aquifer directly overlies the Walloon Coal
61 Measures (WCM), the target coal measures for coal seam gas (CSG) production in the
62 study area. Thus, our study has ramifications for global unconventional gas studies that
63 investigate connectivity issues to freshwater aquifers.

64 Methane is subject to many production and degradation processes in groundwater
65 (Whiticar, 1999). The carbon isotopic composition of CH₄ ($\delta^{13}\text{C-CH}_4$) gives insight into
66 the source (Quay et al., 1999), but oxidation processes may enrich or deplete this
67 signature (Yoshinaga et al., 2014). Therefore, it is very difficult to determine the potential
68 source of CH₄ and processes occurring using CH₄ concentration and isotopic data alone.

69 Previous studies have used geochemical indicators, such as the concentration of
70 sulfate [SO₄²⁻], nitrate [NO₃⁻] and nitrite [NO₂⁻], and the carbon isotopic composition of
71 dissolved inorganic carbon ($\delta^{13}\text{C-DIC}$) and dissolved organic carbon ($\delta^{13}\text{C-DOC}$) to
72 attribute the source of CH₄ in groundwater (Valentine and Reeburgh, 2000; Kotelnikova,
73 2002; Antler, 2014; Green-Saxena et al., 2014; Antler et al., 2015; Hu et al., 2015;



74 Segarra et al., 2015; Sela-Adler et al., 2015; Currell et al., 2016). Other studies have
75 shown that the presence of active methanogenesis can be determined using isotopes of
76 hydrogen in the CH₄ ($\delta^2\text{H-CH}_4$), and the surrounding formation water ($\delta^2\text{H-H}_2\text{O}$)
77 (Schoell, 1980; Whiticar and Faber, 1986; Whiticar, 1999; Currell et al., 2016).
78 Additionally, recent studies have used clumped isotopes of CH₄ and their temperature
79 interpretations to ascribe a thermogenic versus biogenic source in groundwater (Stolper et
80 al., 2014). However, non-equilibrium (kinetic) processes may be responsible for an
81 overestimation of CH₄ formation temperatures (Wang et al., 2015). Therefore, combining
82 geochemistry and microbiology provides a robust method to assess CH₄ origin, as it
83 directly discriminates between microbiological communities involved in either production
84 or degradation processes.

85 Throughout the world the occurrence of freshwater aquifers adjacent to
86 unconventional gas production is common (Osborn et al., 2011; Moore, 2012; Roy and
87 Ryan, 2013; Vidic et al., 2013; Vengosh et al., 2014; Moritz et al., 2015). We have
88 previously shown that there may be local natural connectivity between the WCM and the
89 CRAA (Iverach et al., 2015). Here we show that a combination of geochemical data
90 ([CH₄], [SO₄²⁻], [NO₃⁻], [NO₂⁻], $\delta^{13}\text{C-CH}_4$, $\delta^{13}\text{C-DIC}$, $\delta^{13}\text{C-DOC}$ and $\delta^2\text{H-H}_2\text{O}$), as well as
91 characterisation of microbiological communities present, can inform the discussion
92 surrounding the occurrence of CH₄, and its potential for upward migration in the
93 groundwater of the CRAA.

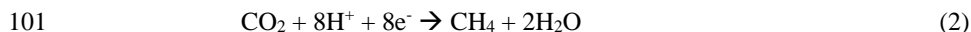
94

95 **1.1 Geochemical indicators of methanogenic processes**

96 Methanogenesis via acetate fermentation (Eq. 1) and carbonate reduction (Eq. 2) can be
97 restricted in groundwater with abundant dissolved SO₄²⁻ (> 19 mg/L) (Whiticar, 1999),



98 because sulfate reducing bacteria (SRB) can outcompete methanogenic archaea for
99 reducing equivalents (Lovley et al., 1985).



102 Therefore, the presence or absence of $[\text{CH}_4]$ and $[\text{SO}_4^{2-}]$ are good preliminary indicators
103 of the potential for methanogenesis.

104 In addition, the $\delta^{13}\text{C}\text{-CH}_4$ of the underlying WCM in the study area has been
105 characterised (Papendick et al., 2011; Hamilton et al., 2012; Hamilton et al., 2014). Thus
106 the isotopic signature can be used to identify the potential source of the CH_4 , however
107 localised formation and oxidation processes that may occur either in the aquifer or during
108 transport can confound the interpretation of mixing versus oxidation processes.

109 The isotopic composition of DIC and DOC are also useful indicators of CH_4
110 processes, as they can be used to determine the occurrence of methanogenesis
111 (Kotelnikova, 2002; Wimmer et al., 2013). Kotelnikova (2002) found that ^{13}C -depletion
112 of $\delta^{13}\text{C}\text{-DOC}$ in combination with a ^{13}C -enrichment of $\delta^{13}\text{C}\text{-DIC}$ was characteristic of
113 methanogenesis in groundwater, consistent with the reduction of $^{12}\text{CO}_2$ by autotrophic
114 methanogens. Conversely, $\delta^{13}\text{C}\text{-DIC}$ data are useful because DIC produced during CH_4
115 oxidation was found to have a characteristically ^{13}C -depleted signature (as depleted as -
116 50‰) (Yoshinaga et al., 2014; Hu et al., 2015; Segarra et al., 2015).

117

118 1.2 Methane oxidation in freshwater

119 In groundwater, CH_4 is oxidised by methane-oxidising bacteria (MOB; methanotrophs)
120 that can utilise CH_4 as their sole carbon and energy source. These methanotrophs are
121 grouped within the *Alpha*- and *Gamma*-Proteobacteria (comprising type I and type II
122 methanotrophs) and the Verrucomicrobia (Hanson and Hanson, 1996). The first step of



123 aerobic CH₄ oxidation is the conversion of CH₄ to methanol. This is catalysed by the
124 particulate CH₄ monooxygenase (*pMMO*) encoded by the *pmoA* gene, which is highly
125 conserved and used as a functional marker (Hakemian and Rosenzweig, 2007; McDonald
126 et al., 2008). All known methanotrophs contain the *pmoA* gene, with members of
127 *Methylocella* the exception (Dedysh et al., 2000; Dunfield et al., 2003). Type II
128 methanotrophs and some type I members of the genus *Methylococcus* contain the *mmoX*
129 gene, which encodes a soluble CH₄ monooxygenase (McDonald et al., 1995; Murrell et
130 al., 2000). Recently, new groups of aerobic and anaerobic MOB distantly related to
131 known methanotrophic groups have been discovered (Raghoebarsing et al., 2006;
132 Stoecker et al., 2006; Op den Camp et al., 2009). Geochemically, aerobic CH₄ oxidation
133 has been previously coupled to denitrification in groundwater (Zhu et al., 2016).

134 Besides methanotrophic bacteria, anaerobic CH₄ oxidising archaea (ANME) also
135 play a significant role in the oxidation of CH₄ in both freshwater and saline water sources
136 (Knittel and Boetius, 2009). These anaerobic methanotrophs are associated with the
137 methanogenic Euryarchaeota within the clusters ANME-1, ANME-2, and ANME-3 and
138 are closely related to the orders *Methanosarcinales* and *Methanomicrobiales* (Knittel et
139 al., 2003; Knittel et al., 2005). Geochemical indicators can provide evidence for the
140 occurrence of AOM, such as the prevalence of certain electron acceptors (SO₄²⁻, NO₃⁻,
141 NO₂⁻ and Fe²⁺) (Valentine and Reeburgh, 2000; Ettwig et al., 2010; Sivan et al., 2011;
142 Antler, 2014; Green-Saxena et al., 2014) and denitrification processes occurring in the
143 groundwater (Ettwig et al., 2008; Nordi and Thamdrup, 2014; Timmers et al., 2015).

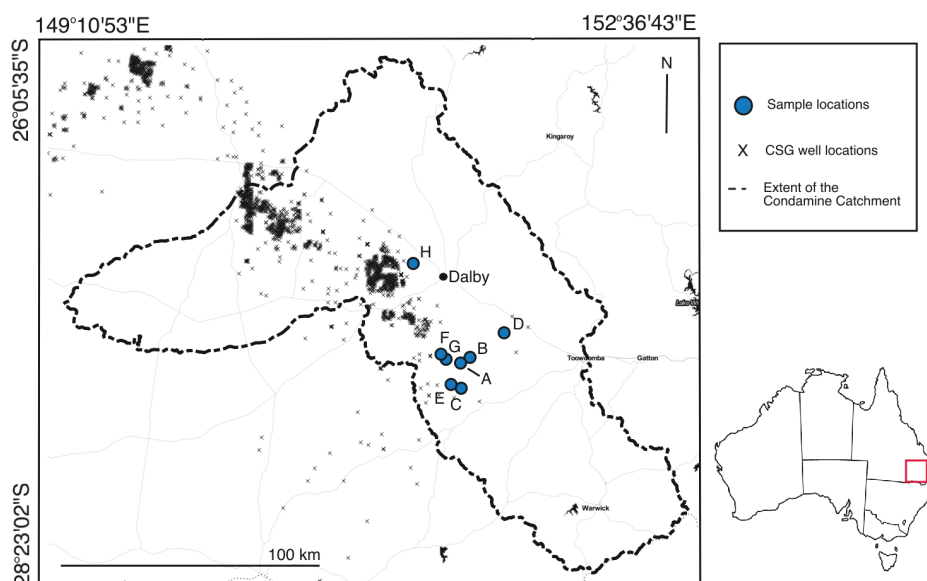
144

145 **2 Study Area**

146 The CRAA is the primary aquifer in the Condamine Catchment (Figure 1). It is used
147 primarily for irrigated agriculture, stock and domestic water supplies. There has been



148 increased interest in the presence of CH₄ in the aquifer due to expanding CSG production
 149 to the north-west of the study area (Figure 1). CSG production began in 2006 (Arrow
 150 Energy, 2015) and has been expanding in the decade since then. This has raised concerns
 151 regarding the quality and quantity of the groundwater in the CRAA.
 152



153
 154 **Figure 1.** Site map showing the extent of the study area and sample locations within the Condamine
 155 Catchment, south-east Queensland, Australia. Map created in QGIS; data and imagery: Stamen Toner, Open
 156 Street Map and contributors, CC-BY-SA (QGIS, 2015). Modified with Corel Painter 2015 (Corel
 157 Corporation, 2015).

158

159 2.1 Hydrogeological setting

160 The CRAA sits within the Surat Basin, which sits within the Great Artesian Basin (GAB)
 161 in south-east Qld, Australia (Figure 1). Aquifers in the GAB vary between semi-confined
 162 and confined (Kelly and Merrick, 2007; Dafny and Silburn, 2014).



163 The environment of deposition for the Surat Basin was fluvio-lacustrine in the late
164 Triassic-Jurassic and shallow marine and coastal in the Cretaceous (Hamilton et al.,
165 2012). The middle-Jurassic WCM are a group of low-rank coal seams in the Surat Basin
166 targeted for CSG production (Hamilton et al., 2012). The WCM are thicker (150 m to 350
167 m) along the western margin of the CRAA and thin to around 50 m in the east, where the
168 unit outcrops (KCB, 2011), however, only around 10 % of this is coal. The unit consists
169 of very fine- to medium-grained sandstone, siltstone, mudstone and coal, with minor
170 calcareous sandstone, impure limestone and ironstone (KCB, 2011). The coal consists of
171 numerous discontinuous thin lenses separated by sediments of low permeability (Hillier,
172 2010). The unit dips gently to the west (around 4°), which is consistent with the general
173 trend of the Surat Basin in this region.

174 The WCM overlie the Eurombah Formation (consisting of conglomerate sandstone
175 with minor siltstones and mudstone beds) and underlie the Kumbarilla Beds (mainly
176 sandstone, with lesser mudstone, siltstones and conglomerates) (KCB, 2011).

177 The unconfined CRAA fills a paleovalley that was carved through the GAB
178 (including the WCM). The valley-filling sediments are composed of gravels and fine- to
179 course-grained channel sands interbedded with floodplain clays and, on the margins,
180 colluvial deposits, which were deposited from the mid-Miocene to the present (Kelly and
181 Merrick, 2007; Kelly et al., 2014). The valley-filling sediments have a maximum
182 thickness of 134 m near Dalby (Dafny and Silburn, 2014). Along the eastern margin of
183 the valley, the CRAA is bounded by the Main Range Volcanics. Estimations of the
184 sources and quantity of recharge to the CRAA vary widely, however streambed recharge
185 is generally considered to be the major source of freshwater to the aquifer (Dafny and
186 Silburn, 2014).



187 A low permeability layer (ranging from 8×10^{-6} to 1.5×10^{-1} m/d) has been reported
188 between the CRAA and the underlying WCM (KCB, 2011; QWC, 2012). This has been
189 referred to as the ‘transition layer’ (QWC, 2012) or a ‘hydraulic basement’ to the
190 alluvium (KCB, 2011). However, the thickness of this layer varies between 30 m thick in
191 some areas to completely absent in others. Thus, in some places the WCM immediately
192 underlies the CRAA (Dafny and Silburn, 2014). This suggests that there is some level of
193 connectivity between the CRAA and the WCM. Huxley (1982) and Hillier (2010) both
194 suggest that the general decline in water quality downstream is due to some net flow of
195 the more saline WCM water into the CRAA. Connectivity between the formations is not
196 well understood; however, studies have been conducted to better understand the
197 movement of both water and gas between the two aquifers. Duvert et al. (2015) and Owen
198 and Cox (2015) both used hydrogeochemical analyses to show that there was limited
199 movement of water between the two formations. However, Iverach et al. (2015) used the
200 isotopic signature of CH_4 in the groundwater to show that there was localised movement
201 of gas between the coal measures and the overlying aquifer. This research provides
202 additional insight to inform the debate about the degree of connectivity between the
203 WCM and the CRAA. The microbiological insights also inform the global research on
204 biological CH_4 production and degradation in alluvial aquifers, in particular for zones
205 distal to the river corridor.

206

207 **3 Methods**

208 From 22 January 2014 to 31 January 2014 we collected groundwater samples for
209 geochemical analysis from 8 private irrigation boreholes in the Condamine Catchment.
210 Iverach et al. (2015) outlines the complete methods for sample collection for $[\text{CH}_4]$ and



211 $\delta^{13}\text{C}\text{-CH}_4$ and subsequent analysis. The 8 samples collected from the unconfined CRAA
212 are representative of the aquifer, given their varied depths and locations.

213 Groundwater samples were collected by installing a sampling tube 2 m inside the
214 pump outlet of the borehole to avoid the air-water interface at the sampling point. Field
215 parameters (electrical conductivity (EC), oxidation-reduction potential (ORP), dissolved
216 oxygen (DO), temperature (T) and pH) were monitored in a flow cell to ensure
217 stabilisation before samples were collected. The boreholes had been pumping
218 continuously over the preceding month for irrigation and so stabilisation of the field
219 parameters was reached within minutes. Groundwater samples for major anions and
220 water-stable isotopes ($\delta^2\text{H}\text{-H}_2\text{O}$ and $\delta^{18}\text{O}\text{-H}_2\text{O}$) were collected after passing the water
221 through a $0.45\ \mu\text{m}$, high-volume groundwater filter, which was connected to the pump
222 outlet. Groundwater for anions and water stable-isotopes were stored in 125 mL high-
223 density polyethylene (HDPE) bottles and 30 mL HDPE bottles, respectively. Both had no
224 further treatment. The water for $\delta^{13}\text{C}\text{-DIC}$ and $\delta^{13}\text{C}\text{-DOC}$ was further filtered through a
225 $0.22\ \mu\text{m}$ filter and stored in 12 mL Exetainer vials and 60 mL HDPE bottles, respectively.
226 Samples to be analysed for DIC were refrigerated at $4\ ^\circ\text{C}$ and samples to be analysed for
227 DOC were frozen within 12 hours of collection.

228 Groundwater samples for the microbiological analyses were collected between 8
229 December 2014 to 11 December 2014, and were collected from the same 8 private
230 irrigation boreholes used for the geochemical analyses. Groundwater samples for
231 microbiological analysis were collected in 2 L Duran Schott bottles and sealed (gas tight).
232 The groundwater was filtered through a $0.2\ \mu\text{m}$ filter (Merck Millipore). We use aspects
233 of the geochemical data collected in the January campaign to inform our interpretation of
234 the microbial results from the December campaign.

235



236 **3.1 Geochemical analyses**

237 The major ion chemistry in the groundwater samples was analysed at the Australian
238 Nuclear Science and Technology Organisation (ANSTO) using Inductively Coupled
239 Plasma - Ion Chromatography for anions. The samples for $\delta^2\text{H-H}_2\text{O}$ and $\delta^{18}\text{O-H}_2\text{O}$ were
240 analysed at ANSTO and are reported as ‰ deviations from the international standard V-
241 SMOW (Vienna Standard Mean Ocean Water). $\delta^{18}\text{O}$ samples were run using an
242 established equilibration, continuous flow IRMS method and $\delta^2\text{H}$ samples were run using
243 an on-line combustion, dual-inlet IRMS method.

244 The isotopes of carbon in DIC were analysed at ANSTO using an established
245 method on a Delta V Advantage mass spectrometer, and a GasBench II peripheral. The
246 results are reported as a ‰ deviation from IAEA secondary standards that have been
247 certified relative to V-PDB for carbon. The isotopes of carbon in DOC were analysed at
248 UC-Davis Stable Isotope Facility and results are reported as ‰ and are corrected based on
249 laboratory standards calibrated against NIST Standard Reference Materials with an
250 analytical precision of $\pm 0.6\%$. Samples were run using a total organic carbon (TOC)
251 analyser connected to a PDZ Europa 20-20 IRMS using a GD-100 Gas Trap interface.
252 The $[\text{SO}_4^{2-}]$ were too low in 6 of the 8 samples for $\delta^{34}\text{S}$ and $\delta^{18}\text{O}$ analysis. The remaining
253 2 samples were analysed for their sulfur and oxygen isotope compositions at the
254 University of Calgary Isotope Science Laboratory. Sulfur isotope ratios were analysed
255 using a Continuous Flow-Isotope Ratio Mass Spectrometry (CF-EA-IRMS) with an
256 elemental analyser interfaced to a VG PRISM II mass spectrometer. The results are
257 reported against V-CDT (Vienna Cañon Diablo Troilite). The oxygen isotope ratio was
258 determined using a high temperature reactor coupled to an isotope ratio mass
259 spectrometer in continuous flow mode.

260



261 **3.2 DNA extraction and Illumina sequencing**

262 DNA was extracted from the biomass collected from filtering 2 L of groundwater. Briefly,
263 DNA was extracted using a phenol-chloroform extraction method as described by Lueders
264 et al. (2004). Subsequently, the DNA was precipitated using polyethylene glycol 6000
265 (Sigma Aldrich), and the DNA pellet was washed using 70 % (v/v) ethanol and
266 resuspended in 50 µL nuclease free water (Qiagen). DNA concentration and purity were
267 determined by standard agarose gel electrophoresis and fluorometrically using RiboGreen
268 (Qubit Assay Kit, Invitrogen) according to the manufacturer's instructions. The extracted
269 DNA was used as a target for Illumina sequencing. Amplicon libraries were generated by
270 following Illumina's 16S Metagenomic Sequencing Library Preparation Protocol, using
271 12.5 ng of template DNA per reaction. The number of cycles for the initial PCR was
272 reduced to 21 to avoid biases from over-amplification. The following universal primer
273 pair was used for the initial amplification, consisting of an Illumina-specific overhang
274 sequence and a locus-specific sequence:

275 926F_Illum(5'-

276 TCGTCGGCAGCGTCAGATGTGTATAAGAGACAG[AAACTYAAAKGAATTGRC
277 CG]-3'),

278 1392R_Illum(5'-

279 GTCTCGTGGGCTCGGAGATGTGTATAAGAGACAG[ACGGGCGGTGTGTRC]-3').

280 This universal primer pair targets the V6-V8 hyper-variable regions of the 16S ribosomal
281 RNA gene and has been shown to capture the microbial diversity of Bacteria and Archaea
282 in a single reaction (Wilkins et al., 2013). PCR products were purified using a magnetic
283 bead capture kit from Agencourt AMPure XP beads (Beckman Coulter) and quantified
284 using a fluorometric kit (RiboGreen, Qubit Assay Kit, Invitrogen). Purified amplicons



285 were subjected to the Index PCR using the MiSeq platform (Ramaciotti Centre for
286 Genomics, UNSW Australia) according to the manufacturer's specifications. Illumina
287 sequences were checked for quality (FastQC, BaseSpace) and analysed using the
288 BaseSpace cloud computing platform (Illumina, 2016) and MOTHUR (Schloss, 2009)
289 with modified protocols (Schloss et al., 2009; Kozich et al., 2013). Taxonomy was
290 assigned against the SILVA Database (Silva, 2016). To ensure even sampling depth for
291 subsequent analyses, OTU abundance data were rarefied to the lowest number of
292 sequences for a sample (8,300 sequences per sample).

293

294 3.3 Quantification of bacterial and archaeal 16S rRNA and functional genes

295 Quantitative real-time PCR was used to determine abundances of bacterial and archaeal
296 16S rRNA gene targets and functional gene targets (*mcrA*, *pmoA*, *mmoX*, and *dsrA*), using
297 the MJ Mini™ 96 Well Thermal Cycler (Bio-Rad, Hercules, CA). Each qPCR 25 µL
298 reaction mixture contained 12.5 µL of premix solution from an iQ SYBRGreen qPCR Kit
299 (Bio-Rad), 8 µL PCR-grade water, 1.5 µL of each primer (final concentration 0.2 – 0.5
300 µM), and 2 µL of template DNA (10 ng). Bacterial and archaeal 16S rRNA genes were
301 amplified using the primer pairs 519F/907R (Lane 1991; Muyzer et al., 1995) and
302 SDArch0025F/SDArch0344R (Vetriani et al., 1999). *McrA* and *dsrA* sequence fragments
303 were amplified using the primer pairs ME1F/ME3R (Hales et al., 1996) and 1F/500R
304 (Wagner et al., 1998; Dhillon et al., 2003). QPCRs were performed as described
305 previously by Wilms et al. (2007). *PmoA* qPCR was performed using the *pmoA* primer-
306 pair A189F (Holmes et al., 1999) and mb661R (Kolb et al., 2003) with a final total
307 concentration of 0.8 µM. The qPCR programme for the amplification was performed as
308 follows: 95°C for 3 min followed by 40 cycles of 95°C for 30 s, 64°C for 45 s and 68°C
309 for 45 s. The *mmoX* gene fragment was quantified using the prime pairs *mmoX*-ms-945f



310 and *mmoXB-1401b* at a final concentration of 0.8 μM . The qPCR conditions for the
311 *mmoX* was as follows: 94°C for 3 min followed by 45 cycles of 94°C for 1 min, 50°C for
312 1 min and 72°C for 1 min. Bacterial and archaeal targets were measured in at least three
313 different dilutions of DNA extracts (1:10, 1:100, 1:1000) and in triplicate. PCR products
314 were checked by gel electrophoresis, using 2 % (w/v) agarose with TBE buffer (90 mM
315 Tris, 90 mM boric acid, 2 mM Na₂-EDTA; pH 8.0). The specificity of the reactions was
316 confirmed by melting curve analysis and agarose gel electrophoresis to identify non-
317 specific PCR products. Amplification efficiencies for all reactions ranged from 96.3 % to
318 110.5 % with an r^2 value of > 0.99 for standard curve regression. DNA calibration
319 standards for qPCR were prepared as follows. The *mcrA*, *dsrA*, *pmoA*, and *mmoX* genes
320 were amplified from pure cultures of *Methanosarcina barkeri*^T (DSM 800), *Desulfovibrio*
321 *vulgaris*^T (DSM 644), *Methylosinus sporium*^T (DSM 17706), and *Methylocella silvestris*^T
322 (DSM 15510; DZMZ Germany). The PCR amplicons were purified using the DNA Clean
323 and ConcentratorTM-5 kit (Zymo Research, Irvine, CA), and eluted into 20 μL DNA
324 elution buffer. DNA concentrations were quantified with 2 μL DNA aliquots using the
325 Qubit® dsDNA BR Assay Kit (Invitrogen, Life Technologies, Carlsbad, CA). Purified
326 target gene PCR products were cloned into plasmids following the manufacturer's
327 instructions for the pGEM® – T Easy Vector System (Promega, Madison, WI).

328

329 **4 Results and Discussion**

330 **4.1 Previous $\delta^{13}\text{C}$ -CH₄ investigation**

331 A previous study by Iverach et al. (2015) analysed the $\delta^{13}\text{C}$ -CH₄ in the groundwater from
332 an off-gassing port on the 8 private irrigation boreholes studied here (samples A-H)
333 (Supplementary Table S3 online). These measurements were understood to have been
334 mixing with regional background atmospheric CH₄ (1.774 ppm; -47‰) and therefore

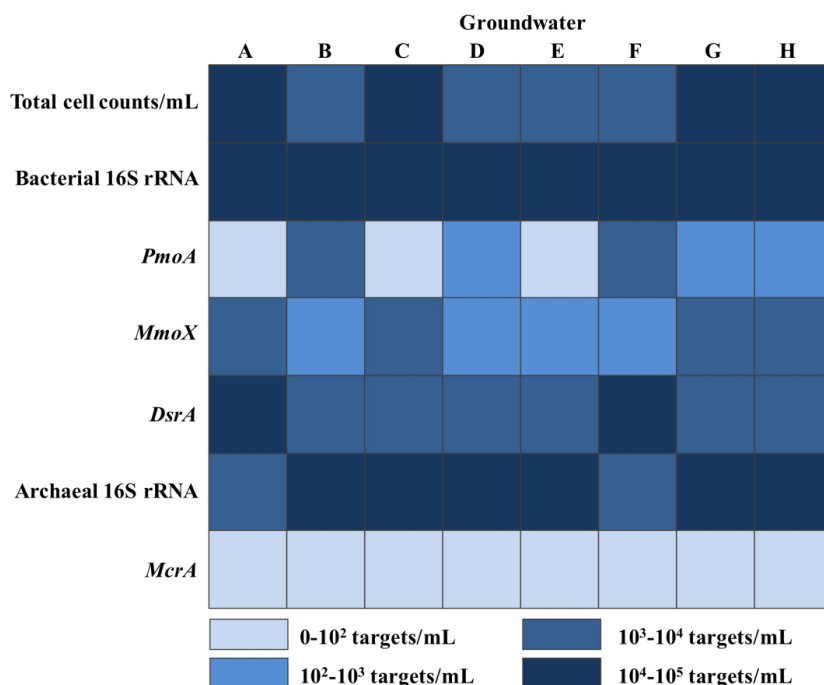


335 mixing plots were used to infer the isotopic source signature of the CH₄ off-gassing from
336 the groundwater. Iverach et al. (2015) found that samples E, G, and H plotted on a
337 regression line that had an isotopic source signature of -69.1‰ (90% CI, -73.2‰ to
338 -65.0‰), indicative of a biological source. However, samples A, B, C, D and F plotted on
339 a regression line that had an isotopic source signature of -55.9‰ (90% CI, -58.3‰ to
340 -53.4‰), suggesting either oxidation was occurring at the source or there was potential
341 upward migration of CH₄ from the underlying WCM.

342

343 **4.2 Limited geochemical and microbiological potential for methanogenesis in the** 344 **groundwater**

345 To further elucidate the source of the CH₄ reported in the groundwater (Iverach et al.,
346 2015), Illumina sequencing and quantitative real-time PCR (qPCR) was used to target
347 bacterial and archaeal 16S rRNA genes, as well as specific functional genes (*mcrA*, *pmoA*,
348 *mmoX* and *dsrA*) associated with CH₄ metabolism. Microbial abundances estimated by
349 SYBR Green I counts were between 10³ and 10⁵ cells/mL throughout all groundwater
350 samples (Figure 2). This was congruent with the qPCR data observed for bacterial and
351 archaeal cell concentrations.



352

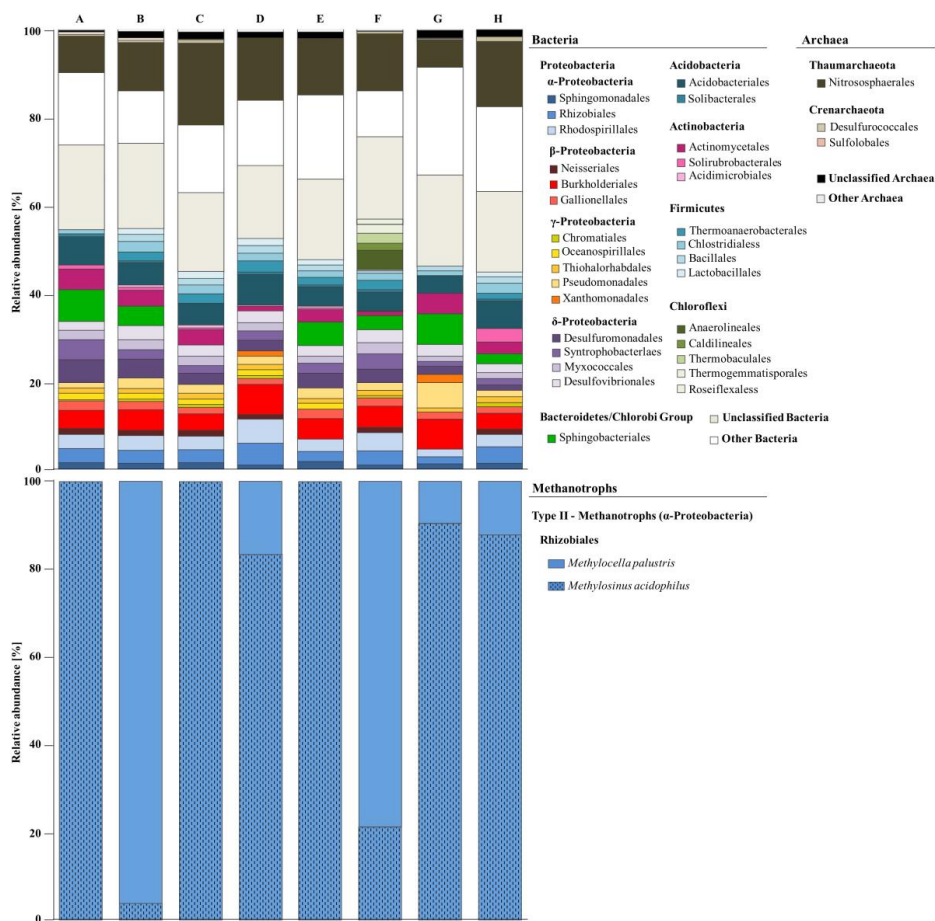
353 **Figure 2.** Total cell concentration and copy number abundances of bacterial and archaeal 16SrRNA genes
 354 and functional key genes for aerobic CH₄ oxidation (*pmoA* and *mmoX* genes), CH₄ production (*mcrA* gene)
 355 and sulfate reduction (*dsrA* gene) in the groundwater carried out by quantitative (q)PCR. Low abundances
 356 are highlighted in light blue. High abundances are highlighted in dark blue.

357

358 The groundwater community was primarily composed of bacteria (79 to 90 %), whilst
 359 archaea made up 10 to 21 % (Figure 3). The bacterial and archaeal community
 360 composition did not vary significantly between groundwater samples. Most of the
 361 bacterial sequences belonged to the phyla Proteobacteria (α - δ), Acidobacteria,
 362 Actinobacteria, Firmicutes and the Bacteroidetes/Chlorobi group (Figure 3). The phylum
 363 Thaumarchaeota dominated the archaeal communities with a relative abundance of 81 to
 364 99 %, while Crenarchaeota made up 1 to 3 % of the archaeal community. Further
 365 sequences were related to other (if < 1 % relative abundance) and unclassified Bacteria
 366 and Archaea. No members of the Euryarchaeota, comprising the methanogenic archaea,



367 were observed. The archaeal *mcrA* gene, which encodes the methyl coenzyme M
 368 reductase, was not detected in any of the groundwater samples (detection limit < 10
 369 cells/mL; Figure 2). This was consistent with the Illumina sequencing results, and
 370 suggests that the CH₄ observed off-gassing from the groundwater was not being produced
 371 locally.

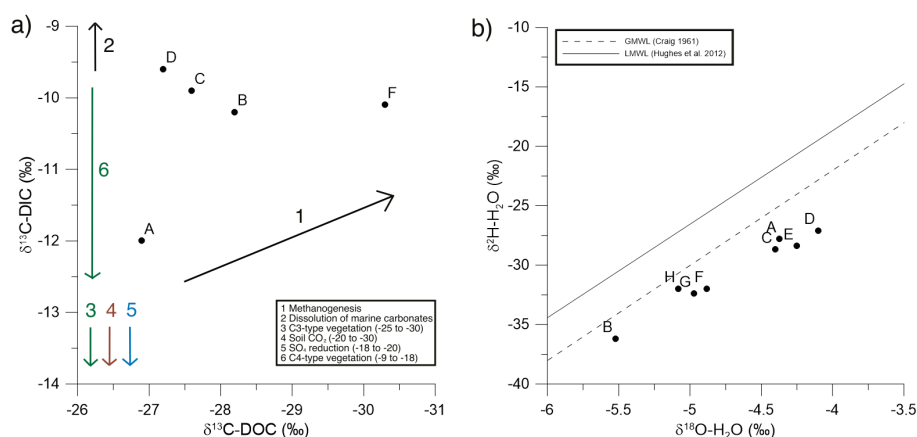


372
 373 **Figure 3.** Bacterial, archaeal, and methanotrophic community profiles and relative abundances detected by
 374 Illumina sequencing.

375
 376 Our geochemical data also showed no evidence for the occurrence of
 377 methanogenesis in the groundwater. As previously stated, a ¹³C-enrichment in δ¹³C-DIC



378 coupled with a ^{13}C -depletion in the $\delta^{13}\text{C}$ -DOC is characteristic of methanogenesis
 379 (Kotelnikova, 2002). Our groundwater data showed no correlation between $\delta^{13}\text{C}$ -DOC
 380 and $\delta^{13}\text{C}$ -DIC (Figure 4a), and the most ^{13}C -enriched $\delta^{13}\text{C}$ -DIC was also the second
 381 highest enriched $\delta^{13}\text{C}$ -DOC value. Additionally, on a stable water isotope plot (Figure 4b;
 382 Supplementary Table S1 online), it is evident that there is no noticeable $\delta^2\text{H}$ -enrichment
 383 that can be ascribed to methanogenesis in any of the groundwater samples (Cendón et al.,
 384 2015).



385

386 **Figure 4.** (a) A plot of $\delta^{13}\text{C}$ -DOC vs. $\delta^{13}\text{C}$ -DIC, highlighting the absence of correlation between these
 387 geochemical data, indicating that there is no methanogenic end member in our samples. Samples E, G and H
 388 are omitted because they were below the detection limit for $\delta^{13}\text{C}$ -DOC (Supplementary Table S1.). Arrow 1
 389 delineates the expected trend for methanogenesis and arrow 2 is the expected trend for the dissolution of
 390 marine carbonates (Currell et al., 2016). Arrows 3-6 highlight expected ranges for $\delta^{13}\text{C}$ -DIC that are off the
 391 scale of the graph (Currell et al., 2016). (b) A plot of $\delta^{18}\text{O}$ - H_2O vs. $\delta^2\text{H}$ - H_2O showing that there is no ^2H -
 392 enrichment in any of the groundwater samples. The GMWL (Craig, 1961) and LMWL (Hughes and
 393 Crawford, 2012) are also displayed.

394

395 These geochemical analyses, along with the lack of classified methanogens, suggest
 396 that biogenic CH_4 production is not one of the major processes producing CH_4 in the
 397 CRAA. Therefore, the CH_4 reported in all samples in Iverach et al. (2015) must be



398 coming from another source. We propose that the upward migration of CH₄ from the
399 WCM must be considered as the potential source. The isotopic signature of CH₄ from the
400 deeper coal measures has been characterised between -58.5‰ and -45.3‰, indicating
401 thermogenic CH₄ with a secondary biogenic component (Papendick et al., 2011; Hamilton
402 et al., 2012; Hamilton et al., 2014). Five of the 8 samples analysed in this study have an
403 isotopic source signature within this range, as reported in Iverach et al. (2015). This
404 implies that upward migration from the deeper WCM is the source of the CH₄ detected in
405 the groundwater.

406 However, the remaining 3 samples (samples E, G, and H) have a typically biogenic
407 isotopic source signature (-69.1‰). This could be the result of the replacement of
408 typically thermogenic gas in the shallow WCM by biogenic gas (Faiz and Hendry, 2006).
409 Thus, these three sites are potentially sourcing biogenic CH₄ from the shallow WCM,
410 resulting in a biological source signature despite the absence of methanogens in the
411 overlying aquifer.

412

413 **4.3 Sulfate reducers and aerobic methanotrophs potentially outcompete** 414 **methanogens**

415 Sulfate concentrations in most groundwater samples were low (3.2 mg/L to 11 mg/L)
416 (Supplementary Table S2 online). Groundwater samples D and H were higher with 55
417 mg/L and 29 mg/L, respectively (Supplementary Table S2 online). Sequence and
418 functional *dsrA* gene analysis (encoding the dissimilatory sulfite reductase of SRB)
419 revealed that SRB are present in all groundwater samples at relatively high abundances (5
420 - 10 % of the overall microbial community; Figures 2 and 3). These SRB are potentially
421 outcompeting methanogenic archaea for substrates such as acetate and H₂. Sulfate
422 concentrations higher than 3 mg/L, as detected in all groundwater samples (3.2 mg/L – 55



423 mg/L), could potentially create a SO_4^{2-} -reducing environment with the predominance of
424 SRB over methanogens. This would maintain the acetate at concentrations too low for
425 methanogens to grow (Lovley et al., 1985). Deltaproteobacteria were dominant in all
426 groundwater samples, and most of the sequences were closely related to acetate-oxidising,
427 sulfate/sulfur-reducing bacteria (*Desulfovibrionales*, *Syntrophobacterales*,
428 *Desulfuromonadales*; Figure 3). Additionally, *Methylocella* spp. are capable of using
429 methanogenic substrates, such as acetate and methylamines, for their metabolism and
430 therefore are not limited to growing on one-carbon compounds such as CH_4 (Dedysh et
431 al., 2005). This could have major implications for the lack of methanogenic activity in the
432 groundwater.

433

434 **4.4 Microbial methane oxidation in the groundwater catalyses upward migrating** 435 **methane from the WCM**

436 The functional gene for aerobic CH_4 oxidation (*pmoA*) was detected at relatively high
437 concentrations (7.9×10^2 - 9.3×10^3 targets/mL) compared to the overall bacterial 16S
438 rRNA concentration (2.5×10^4 - 5.1×10^4 targets/mL) (Figure 2). All groundwater
439 samples were characterised with regard to the community structure of MOB. The samples
440 harboured a low-diversity methanotrophic community associated with the order
441 *Rhizobiales* (α -Proteobacteria), however MOB accounted for up to 7 % of the overall
442 microbial community (Figure 3). All groundwater samples were dominated by two MOB,
443 belonging to the type II methanotrophs (Figure 3). Five samples had both *Methylocella*
444 *palustris* (family *Beijerinckiaceae*) and *Methylosinus acidophilus* (family
445 *Methylocystaceae*) (samples B, D, F-H), whilst the remaining samples comprised
446 *Methylosinus acidophilus* only (samples A, C and E) (Figure 3). These genera were
447 characterised as aerobic CH_4 oxidisers, however aerobic MOB have been previously



448 observed in micro-aerophilic and anaerobic environments (Bowman, 2000). This suggests
449 the existence of an alternative pathway for aerobic CH₄ oxidation in a suboxic/anaerobic
450 environment. Both species have previously been found and isolated from a variety of
451 freshwater habitats and *Methylosinus* spp. are known to be dominant methanotrophic
452 populations in groundwater (Bowman, 2000). *Methylocella* and *Methylosinus* spp. possess
453 a soluble CH₄ monooxygenase (*mmoX*) (McDonald et al., 1995; Murrell et al., 2000),
454 which is consistent with the high abundance of the *mmoX* gene targeted in all
455 groundwater samples (Figure 2). Interestingly, no *pmoA* gene, a biomarker for all MOB_s,
456 has previously been detected in known *Methylosinus* spp. (Dedysh et al., 2005). This is
457 supported by our data, which shows the sole predominance of *mmoX* genes in 3 of the 8
458 groundwater samples that are exclusively dominated by *Methylosinus* sp. (samples A, C,
459 and E) (Figures 2 and 3).

460 In addition to low concentrations of CH₄ reported in Iverach et al. (2015), the
461 dissolved O₂ (DO) in our groundwater samples had a large range, from low to close to
462 saturation (0.91 mg/L to 8.6 mg/L). *Methylocella* spp. are not associated with the
463 previously known type II cluster of methanotrophs, but are closely related to a non-
464 methanotroph (Dedysh et al., 2005) suggesting different affinities to CH₄ and O₂,
465 compared to previously known type II methanotrophs (Amaral and Knowles, 1995).
466 There is no correlation between the methanotrophic community in each sample and the
467 CH₄ data reported in Iverach et al. (2015), nor is there any correlation between the
468 composition of methanotrophs and DO in the groundwater (Supplementary Table S2
469 online).

470 The sample with the most diverse bacterial community (Sample F; Figure 3) had the
471 most ¹³C-enriched individual δ¹³C-CH₄ relative to regional background (Iverach et al.,
472 2015) (Supplementary Table S3 online). A relatively high abundance (11 %) of relatives



473 belonging to the Chloroflexi phylum was observed exclusively in this groundwater
474 sample. This suggests that there are potential metabolic processes involved, such as the
475 microbial conversion of denitrification products to nitrogen and oxygen, that are able to
476 gain oxygen to facilitate the oxidation of CH₄ (Ettwig et al., 2010).

477

478 **4.5 Absence of AOM**

479 The lack of detection of the *mcrA* gene does not only indicate the absence of methanogens
480 but also suggests the absence of anaerobic methanotrophs (Hallam et al., 2003). Details
481 on the functional genomic link between methanogenic and methanotrophic archaea are
482 discussed comprehensively in Hallam et al. (2003). Additionally, no sequences belonging
483 to ANME-SRB clades were detected in the groundwater samples, indicating the absence
484 of ANME activity. However, members of the phylum Thaumarchaeota dominated the
485 archaeal community in the groundwater (Figure 3). Thaumarchaeota contains several
486 clusters of environmental sequences representing microorganisms with unknown energy
487 metabolism (Pester et al., 2011). Members of the Thaumarchaeota encode
488 monooxygenase-like enzymes able to utilise CH₄, suggestive of a role in CH₄ oxidation.

489 Samples D and H had SO₄²⁻ concentrations of 55 mg/L and 29 mg/L, respectively.
490 This suggests that the SO₄²⁻ concentration is high enough to support SO₄²⁻-mediated AOM
491 at these sites (Whiticar, 1999). The observed [SO₄²⁻] was high enough in these 2 samples
492 to be able to measure the stable isotopes in the SO₄²⁻. This is useful because the isotopes
493 yield a unique signature when SO₄²⁻ reduction is coupled to CH₄ oxidation in anaerobic
494 conditions (Antler et al., 2015). However, because there are only two data points
495 (Supplementary Table S2 online), determining a correlation between δ³⁴S-SO₄ and δ¹⁸O-
496 SO₄ is statistically invalid. The highest relative abundance of methanotrophs was found in



497 samples D and H (Figure 3); however, these methanotrophs are not anaerobic oxidisers
498 and therefore the correlation may not imply causation.

499 The concentration of NO_3^- and NO_2^- in the groundwater was also very low, with
500 $[\text{NO}_3^-]$ ranging from 1.2 mg/L to 2.3 mg/L and for all samples NO_2^- was below 0.05 mg/L
501 (Supplementary Table S2 online). Therefore, AOM coupled to denitrification is unlikely
502 to be occurring in the groundwater of the CRAA (Nordi and Thamdrup, 2014).

503 The $\delta^{13}\text{C}$ -DIC data indicates limited ^{13}C -depletion as a result of DIC formation
504 during AOM. Segarra et al. (2015) showed that maximum ^{13}C -depletion of DIC in the
505 zone of maximum AOM activity (0 – 3 cm) was highly dependent upon the isotopic
506 composition of the DIC before biological consumption. However, the difference between
507 maximum ^{13}C -depletion of DIC and ^{13}C -enrichment often exceeded 10‰. As our samples
508 are taken from deep in the aquifer (30 m or more below the ground surface), and the
509 difference between our most ^{13}C -depleted DIC value and the most ^{13}C -enriched was only
510 4‰ (Sample H; Supplementary Table SI online) it is unlikely that AOM is occurring in
511 the groundwater. Additionally, a previous study of the GAB geochemistry showed that
512 $\delta^{13}\text{C}$ -DIC values in this region are in the range -15‰ to -6‰ (Herczeg et al., 1991). All of
513 our samples fall within this regional range, and we see no obvious ^{13}C -depletion of DIC in
514 the groundwater that can be ascribed to AOM.

515 Therefore, any oxidation occurring in the groundwater would have been facilitated
516 by the two members of type II methanotrophs that we identified in the microbial
517 community analysis. Both of the species identified are classified aerobic CH_4 oxidisers,
518 agreeing with our geochemical data that no anaerobic oxidation was occurring. Despite
519 abundant SO_4^{2-} in 2 sample locations, the absence of anaerobic methanotrophic archaea
520 amongst other geochemical evidence (denitrification processes) suggests that it is unlikely
521 that AOM is occurring within the aquifer.



522

523 **5 Conclusion**

524 We used geochemical and microbiological indicators to explain the occurrence of CH₄ in
525 the groundwater of an alluvial aquifer. Microbial community analysis and geochemical
526 data were consistent with respect to a lack of methanogenic archaea and methanogenic
527 activity in the aquifer. What is the original source of the CH₄ if not biologically produced
528 *in-situ*? One hypothesis to explain the presence of CH₄ despite there being no evidence of
529 methanogenesis is that there is localised upward migration of CH₄ from the WCM into the
530 CRAA via natural faults and fractures (Iverach et al., 2015).

531 Our geochemical data and microbiological community analysis both indicate that
532 AOM is not a major oxidation process occurring in the CRAA. However, the
533 microbiological data suggest the presence of aerobic CH₄ oxidisers. Due to the absence of
534 methanogenesis, the oxidation of CH₄ (facilitated by the aerobic methanotrophs present in
535 the groundwater) would require a secondary source of CH₄. The upwards migration of
536 CH₄ from the underlying WCM is the likely source.

537 Methane occurs naturally in groundwater, is produced via numerous biological
538 pathways, and can migrate through natural geological fractures. Therefore, determination
539 of the source of CH₄ using [CH₄] and δ¹³C-CH₄ data alone doesn't discern all the
540 processes occurring. Our microbiological community analysis showed that there were no
541 methanogens present to produce the CH₄ measured in Iverach et al. (2015) and our
542 geochemical analyses supported the absence of methanogenesis in the alluvial aquifer.
543 Similarly, the geochemical and microbiological data revealed that oxidation may not have
544 as large an effect on the CH₄ due to the low abundance of aerobic oxidisers and the
545 absence of anaerobic archaea.



546 Therefore, we suggest that the CH₄ detected in the CRAA in Iverach et al. (2015) is
547 from the local upward migration of gas from the underlying WCM, through natural faults
548 and fractures. A consideration of both geochemical and microbiological analyses is
549 particularly important in this study area because of the immediate proximity of the
550 underlying WCM and the proximity of the study area to CSG production. This research
551 uses biogeochemical constraints on the origin of CH₄ in a freshwater aquifer to
552 demonstrate the upward migration of CH₄ from an underlying coal seam.

553 **Author Contributions**

554 Experimental conceptualisation and design was carried out by D.I.C. & B.F.J.K.
555 Fieldwork was conducted by C.P.I., S.B., D.I.C. & B.F.J.K. Geochemical analyses were
556 conducted by D.I.C. Microbiological analyses were conducted by S.B., C.P.I. & M.M.
557 The manuscript was written by C.P.I. and S.B. with input from all authors.

558

559 **Acknowledgements**

560 This research was funded by the Cotton Research and Development Corporation and the
561 National Centre for Groundwater Research and Training (funded by the Australian
562 Research Council and the National Water Commission).

563 **Competing Interests**

564 The authors declare that they have no conflict of interest.

565 **List of Figures**

566 **Figure 1.** Site map showing the extent of the study area and sample locations within the
567 Condamine Catchment, south-east Queensland, Australia. Map created in QGIS; data and



568 imagery: Stamen Toner, Open Street Map and contributors, CC-BY-SA (QGIS, 2015).

569 Modified with Corel Painter 2015 (Corel Corporation, 2015).

570 **Figure 2.** Total cell concentration and copy number abundances of bacterial and archaeal

571 16SrRNA genes and functional key genes for aerobic CH₄ oxidation (*pmoA* and *mmoX*

572 genes), CH₄ production (*mcrA* gene) and sulfate reduction (*dsrA* gene) in the groundwater

573 carried out by quantitative (q)PCR. Low abundances are highlighted in light blue. High

574 abundances are highlighted in dark blue.

575 **Figure 3.** Bacterial, archaeal, and methanotrophic community profiles and relative

576 abundances detected by Illumina sequencing.

577 **Figure 4.** (a) A plot of $\delta^{13}\text{C-DOC}$ vs. $\delta^{13}\text{C-DIC}$, highlighting the absence of correlation

578 between these geochemical data, indicating that there is no methanogenic end member in

579 our samples. Samples E, G and H are omitted because they were below the detection limit

580 for $\delta^{13}\text{C-DOC}$ (Supplementary Table S1.). Arrow 1 delineates the expected trend for

581 methanogenesis and arrow 2 is the expected trend for the dissolution of marine carbonates

582 (Currell et al., 2016). Arrows 3-6 highlight expected ranges for $\delta^{13}\text{C-DIC}$ that are off the

583 scale of the graph (Currell et al., 2016). (b) A plot of $\delta^{18}\text{O-H}_2\text{O}$ vs. $\delta^2\text{H-H}_2\text{O}$ showing that

584 there is no ²H-enrichment in any of the groundwater samples. The GMWL (Craig, 1961)

585 and LMWL (Hughes and Crawford, 2012) are also displayed.

586

587 **6 References**

588 Amaral, J.A., & Knowles, R. Growth of methanotrophs in methane and oxygen counter gradients. FEMS
589 Microbiol. Let. 126, 215-220, (1995).

590

591 Antler, G. Sulfur and oxygen isotope tracing of sulfate driven anaerobic methane oxidation in estuarine
592 sediments. Estuar. Coast. Shelf Sci. 142, 4-11, (2014).

593

594 Antler, G., Turchyn, A.V., Herut, B. & Sivan, O. A unique isotopic fingerprint of sulfate-driven anaerobic
595 oxidation of methane. Geology 43(7), 619-622, (2015).



596
597 Arrow Energy, Our Operations (2015). Available at: [http://www.arrowenergy.com.au/our-company/our-](http://www.arrowenergy.com.au/our-company/our-projects)
598 [projects](http://www.arrowenergy.com.au/our-company/our-projects) (Accessed: 18 May 2016).
599
600 Atkins, M.L., Santos, I.R. & Maher, D.T. Groundwater methane in a potential coal seam gas extraction
601 region. *J. Hydrology: Reg. Stud.* 4(B), 452-471, (2015).
602
603 Barker, J.F. & Fritz, P. The occurrence and origin of methane in some groundwater flow systems. *Can. J. of*
604 *Earth Sci.* 18(12), 1802-1816, (1981).
605
606 Bowman, J. (2000) The Methanotrophs: the families Methylococcaceae and Methylocystaceae. In *The*
607 *Prokaryotes, an evolving Electronic Resource for the Microbiological Community.* Dworkin, M., Falkow,
608 S., Rosenberg, E., Schleifer, K.-H., and Stackebrandt, E. (eds). Heidelberg: Springer Science Online.
609 (www.prokaryotes.com)
610
611 Cendón, D. I., Hughes, C. E., Harrison, J. J., Hankin, S. I., Johansen, M. P., Payne, T. E., Wong, H.,
612 Rowling, B., Vine, M., Wilsher, K., Guinea, A., & Thiruvoth, S. Identification of sources and processes in a
613 low-level radioactive waste site adjacent to landfills: groundwater hydrogeochemistry and isotopes. *Aus. J.*
614 *Earth Sci.* 62(1), 123-141, (2015).
615
616 Corel Corporation, Corel Painter Education, Version 14.1.0.1105, 2015.
617
618 Craig, H. Isotopic variations in meteoric waters. *Science.* 133 (3465), 1702-1703, (1961).
619 Dafny, E. & Silburn, D.M. The hydrogeology of the Condamine River Alluvial Aquifer, Australia: a critical
620 assessment. *Hydrogeol. J.* 22, 705-727, (2014).
621
622 Currell, M., Banfield, D., Cartwright, I. & Cendón, D.I. Geochemical indicators of the origins and evolution
623 of methane in groundwater: Gippsland Basin, Australia, *Environ. Sci. Pollut. Res.* DOI 10.1007/s11356-
624 016-7290-0
625
626 Dafny, E. & Silburn, D. M. The hydrogeology of the Condamine River Alluvial Aquifer, Australia: a
627 critical assessment. *Hydrogeol. J.* 22, 705-727, (2014).
628
629 Dedysh, S.N. et al. *Methylocella palustris* gen. nov., sp. nov., a new methane-oxidizing acidophilic
630 bacterium from peat bogs, representing a novel subtype of serine-pathway methanotrophs. *Int. J. Syst. Evol.*
631 *Microbiol.* 50, 955-969, (2000).
632
633 Dedysh, S.N., Knief, C. & Dunfield, P.F. *Methylocella* species are facultatively methanotrophic. *J.*
634 *Bacteriol.* 187, 4665-4670, (2005).
635



- 636 Dhillon, A., Teske, A., Dillon, J., Stahl, D.A. & Sogin, M.L. Molecular characterization of sulfate-reducing
637 bacteria in the Guaymas basin. *Appl. Environ. Microbiol.* 69, 2765-2772, (2003).
638
- 639 Dunfield, P.F., Khmelenina, V.N., Suzina, N.E., Trotsenko, Y.A. & Dedysh, S.N. *Methylocella silvestris* sp.
640 nov., a novel methanotrophic bacterium isolated from an acidic forest cambisol. *Int. J. Syst. Evol.*
641 *Microbiol.* 53, 1231-1239, (2003).
642
- 643 Duvert, C., Raiber, M., Owen, D.D.R., Cendón, D.I., Batiot-Guilhe, C. & Cox, M.E. Hydrochemical
644 processes in a shallow coal seam gas aquifer and its overlying stream-alluvial system: implications for
645 recharge and inter-aquifer connectivity. *Appl. Geochem.* 61, 146-159, (2015).
646
- 647 Ettwig, K.F., Shima, S., van de Pas-Schoonen, K.T., Kahnt, J., Medema, M.H., Op den Camp, H.J.M.,
648 Jetten, M.S.M. & Storus, M. Denitrifying bacteria anaerobically oxidize methane in the absence of Archaea.
649 *Environ. Microbiol.* 10(11), 3164-3173, (2008).
650
- 651 Ettwig, K.F. et al. Nitrite-driven anaerobic methane oxidation by oxygenic bacteria. *Nature* 464, 543-548,
652 (2010).
653
- 654 Faiz, M. & Hendry, P. Significance of microbial activity in Australian coal bed methane reservoirs – a
655 review. *Bull. Can. Pet. Geol.* 54(3), 261-272, (2006).
656
- 657 Fontenot, B.E., Hunt, L.R., Hildenbrand, Z.L., Carlton Jr, D.D., Oka, H., Walton, J.L., Hopkins, D., Osorio,
658 A., Bjorndal, B., Hu, Q.H. & Schug, K.A. An evaluation of water quality in private drinking water wells
659 near natural gas extraction sites in the Barnett Shale Formation. *Environ. Sci. Tech.* 47, 10032-10040,
660 (2013).
661
- 662 Green-Saxena, A., Dekas, A.E., Daleska, N.F. & Orphan, V.J. Nitrate-based niche differentiation by distinct
663 sulfate-reducing bacteria involved in the anaerobic oxidation of methane. *ISME J.* 8, 150-163, (2014).
664
- 665 Hakemian, A.S. & Rosenzweig, A.C. The biogeochemistry of methane oxidation. *Ann. Rev. Biochem.* 76,
666 223-241, (2007).
667
- 667 Hales, B.A., Edwards, C., Ritchie, D.A., Hall, G., Pickup, R.W. & Saunders, J.R. Isolation and
668 identification of methanogen-specific DNA from blanket bog peat by PCR amplification and sequence
669 analysis. *Appl. Environ. Microbiol.* 62, 668-675, (1996).
670
- 671 Hallam, S.J., Girguis, P.R., Preston, C.M., Richardson, P.M., DeLong, E.F. (2003) Identification of methyl
672 coenzyme M reductase A (*mcrA*) genes associated with methane-oxidising archaea. *Applied and*
673 *Environmental Microbiology*. Vol. 69, 5483-5491.
674



- 675 Hamilton, S.K., Esterle, J.S. & Golding, S.D. Geological interpretation of gas content trends, Walloon
676 Subgroup, eastern Surat Basin, Queensland, Australia. *Int. J. Coal. Geol.* 101, 21-35, (2012).
677
- 678 Hamilton, S.K., Golding, S.D., Baublys, K.A. & Esterle, J.S. Stable isotopic and molecular composition of
679 desorbed coal seam gas from the Walloon Subgroup, eastern Surat Basin, Australia. *Int. J. Coal Geol.* 122,
680 21-36, (2014).
681
- 682 Hanson, R.S. & Hanson, T.E. Methanotrophic bacteria. *Microbiol. Rev.* 60, 439-471, (1996).
683
- 684 Heilweil, V.M., Grieve, P.L., Hynek, S.A., Brantley, S.L., Solomon, D.K. & Risser, D.W. Stream
685 measurements locate thermogenic methane fluxes in groundwater discharge in an area of shale-gas
686 development. *Env. Sci. Tech.* 49(7), 4057-4065, (2015).
687
- 688 Herczeg, A.L., Torgersen, T., Chivas, A.R. & Habermehl, M.A. Geochemistry of ground waters from the
689 Great Artesian Basin, Australia. *J. Hydrol.* 126, 225-245, (1991).
690
- 691 Hillier, J.R. Groundwater connections between the Walloon Coal Measures and the Alluvium of the
692 Condamine River. Central Downs Irrigators Limited, Bribie Island, Queensland, Australia, (2010).
693
- 694 Holmes, A.J., Roslev, P., McDonald, I.R., Iversen, N., Henriksen, K. & Murrell, J.C. Characterisation of
695 methanotrophic bacterial populations in soils showing atmospheric methane uptake. *Appl. Environ.*
696 *Microbiol.* 65, 3312-3318, (1999).
697
- 698 Hu, Y., Feng, D., Liang, Q., Xia, Z., Linying, C. & Chen, D. Impact of anaerobic oxidation of methane on
699 the geochemical cycle of redox-sensitive elements at cold-seep sites of the northern South China Sea. *Deep-*
700 *Sea Res. II* 122, 84-94, (2015).
701
- 702 Hughes, C.E. & Crawford, J. A new precipitation weighted method for determining the meteoric water line
703 for hydrological applications demonstrated using Australian and global GNIP data. *J. Hydrol.* 464-465, 344-
704 351, (2012).
705
- 706 Huxley, W.J. Condamine River valley groundwater investigation: the hydrogeology, hydrology and
707 hydrochemistry of the Condamine River valley alluvium. Queensland Water Resources Commission,
708 Brisbane, Australia. (1982).
709
- 710 Illumina, Basespace Sequence Hub (2016). Available at: <http://basespace.illumina.com> (Accessed 3 May
711 2016).
712



713 Iverach, C.P., Cendón, D.I., Hankin, S.I., Lowry, D., Fisher, R.E., France, J.L., Baker, A. & Kelly, B.F.J.
714 Assessing connectivity between an overlying aquifer and a coals seam gas resource using methane isotopes,
715 dissolved organic carbon and tritium. *Sci. Rep.* 5, 1-11, (2015).
716
717 KCB (Klohn Crippen Berger), Conceptualisation of the Walloon Coal Measures beneath the Condamine
718 Alluvium – Final Report. Dept. of Environment and Resource Management, Toowoomba, Queensland,
719 Australia, (2011).
720
721 Kelly, B.F.J. & Merrick, N. Groundwater Knowledge and Gaps in the Condamine Alliance Area for the
722 Cotton Catchment Communities CRC, UTS – National Centre for Groundwater Management Report,
723 NCGM, (2007).
724
725 Kelly, B.F.J., Timms, W., Ralph, T.J., Giambastiani, B.M.S., Comunian, A., McCallum, A.M., Andersen,
726 M.S., Blakers, R.S., Acworth, R.I. & Baker, A. A reassessment of the Lower Namoi Catchment aquifer
727 architecture and hydraulic connectivity with reference to climate drivers. *Aust. J. Earth Sci.* 61(3), 501-511,
728 (2014).
729
730 Knittel, K., Boetius, A., Lemke, A., Eilers, H., Lochte, K., Pfannkuche, O., Linke, P. & Amann, R. Activity,
731 distribution, and diversity of sulfate reducers and other bacteria in sediments above gas hydrate (Cascadia
732 margin, Oregon). *Geomicrobiol. J.* 20, 269-294, (2003).
733
734 Knittel, K., Loesekann, T., Boetius, A., Kort, R. & Amann, R. Diversity and distribution of methanotrophic
735 archaea at cold seeps. *Appl. Environ. Microbiol.* 71, 467-479, (2005).
736
737 Knittel, K. & Boetius, A. Anaerobic oxidation of methane: progress with an unknown process. *Annu. Rev.*
738 *Microbiol.* 63, 311-334, (2009).
739
740 Kolb, S., Knief, C., Stubner, S & Conrad, R. Quantitative detection of methanotrophs in soil by novel
741 pmoA-targeted real-time PCR assays. *Appl. Environ. Microbiol.* 69, 2423-2429, (2003).
742
743 Kotelnikova, S. Microbial production and oxidation of methane in deep subsurface. *Earth-Sci Rev.* 58, 367-
744 395, (2002).
745
746 Kozich, J.J., Westcott, S.L., Baxter, N.T., Highlander, S.K. & Schloss, P.D. Development of a dual-index
747 sequencing strategy and curation pipeline for analysing amplicon sequence data on the MiSeq Illumina
748 sequencing platform. *Appl. Environ. Microbiol.* 79, 5112-5120, (2013).
749
750 Lane, D.J. 16S/23S sequencing. In Stackebrandt, E. & Goodfellow, M. *Nucleic Acid Techniques in*
751 *Bacterial Systematics*, Wiley, Chichester, 205-248, (1991).
752



- 753 Lovley, D.R. et al. Model for the distribution of sulfate reduction and methanogenesis in freshwater
754 sediments. *Geochim. et Cosmochim. Acta* 50, 11-18, (1985).
755
- 756 Lueders, T., Manefield, M. & Friedrich, M.W. Enhanced sensitivity of DNA-and rRNA-based stable
757 isotope probing by fractionation and quantitative analysis of isopycnic centrifugation gradients. *Environ.*
758 *Microbiol.* 6, 73-78, (2004).
759
- 760 McDonald, L.R., Kenna, E.M. & Murrell, J.C. Detection of methanotrophic bacteria in environmental
761 samples with the PCR. *Appl. Environ. Microbiol.* 61, 116-121, (1995).
762
- 763 McDonald, I.R., Bodrossy, L., Chen, Y. & Murrell, J.C. Molecular ecology techniques for the study of
764 aerobic methanotrophs. *Appl. Environ. Microbiol.* 74, 1305-1315, (2008).
765
- 766 Moore, T.A. Coalbed methane: a review. *Int. J. Coal Geol.* 101, 36-81, (2012).
767
- 768 Mortiz, A., Hélie, J.F., Pinti, D.L., Larocque, M., Barnetche, D., Retailleau, S., Lefebvre, R. & Gélinas, Y.
769 Methane baseline concentrations and sources in shallow aquifers from the shale gas-prone region of the St.
770 Lawrence Lowlands (Quebec, Canada). *Env. Sci. Tech.* 49(7), 4765-4771, (2015).
771
- 772 Murrell, J.C., Gilbert, B. & McDonald, I.R. Molecular biology and regulation of methane monooxygenase.
773 *Arch. Microbiol.* 173, 325-332, (2000).
774
- 775 Muyzer, G., Teske, A., Wirsén, C.O. & Jannasch, H.W. Phylogenetic relationships of *Thiomicrospira*
776 species and their identification in deep-sea hydrothermal vent samples by denaturing gel electrophoresis of
777 16S rDNA. *Arch. Microbiol.* 164, 165-172, (1995).
778
- 779 Nordi, K. & Thamdrup, B. Nitrate-dependent anaerobic methane oxidation in a freshwater sediment.
780 *Geochim. et Cosmochim. Acta* 132, 141-150, (2014).
781
- 782 Papendick, S.L. et al. Biogenic methane potential for Surat Basin, Queensland coal seams. *Int. J. Coal Geol.*
783 88, 123-134, (2011).
784
- 785 Pester, M., Schleper, C., Wagner, M. (2011) The Thaumarchaeota: an emerging view of their phylogeny
786 and ecophysiology. *Current Opinion in Microbiology*, 14: 300-306.
787
- 788 Op den Camp, H.J.M. et al. Environmental, genomic and taxonomic perspectives on methanotrophic
789 *Verrucomicrobia*. *Environ. Microbiol. Rep.* 1, 293-306, (2009).
790



- 791 Osborn, S.G., Vengosh, A., Warner, N.R. & Jackson, R.B. Methane contamination of drinking water
792 accompanying gas-well drilling and hydraulic fracturing. *Proc. Natl. Acad. Sci. USA.* 108, 8172-8176,
793 (2011).
- 794
- 795 Owen, D.D.R. & Cox, M.E. Hydrochemical evolution within a large alluvial groundwater resource
796 overlying a shallow coal seam gas reservoir. *Sci. Tot. Environ.* 523, 233-252, (2015).
797
- 798 Queensland Water Commission (QWC). Underground water impact report: Surat cumulative management
799 area. QWC, Brisbane, Australia, (2012).
800
- 801 QGIS 2.8.2 Wien, 2015, Stamen Toner and Open Street Map licensed under Creative Commons Attribution
802 – ShareAlike 3.0 license (CC-BY-SA).
803
- 804 Quay, P. et al. The isotopic composition of atmospheric methane. *Glob. Biogeochem. Cycles* 13, 445-461,
805 (1999).
806
- 807 Raghoebarsing, A.A. et al. A microbial consortium couples anaerobic methane oxidation to denitrification.
808 *Nature* 440, 918-921, (2006).
809
- 810 Roy, J.W. & Ryan, M.C. Effects of unconventional gas development on groundwater: a call for total
811 dissolved gas pressure field measurements. *Groundwater.* 51(4), (2013).
- 812
- 813 Schloss, P.D., mothur (2009). Available at: <http://www.mothur.org/> (Accessed 3 May 2016).
814
- 815 Schloss, P.D. et al. Introducing MOTHUR: open-source, platform-independent, community-supported
816 software for describing and comparing microbial communities. *Appl. Environ. Microbiol.* 75, 7537-7541,
817 (2009).
818
- 819 Schoell, M. The hydrogen and carbon isotopic composition of methane from natural gases of various
820 origins. *Geochim. et Cosmo. Acta* 44(5), 649-661, (1980).
821
- 822 Segarra, K.E.A., Schubotz, F., Samarkin, V., Yoshinaga, M.Y., Hinrichs, K-U. & Joye, S.B. High rates of
823 anaerobic methane oxidation in freshwater wetlands reduce potential atmospheric methane emissions. *Nat.*
824 *Commun.* 6:7477, 1-8, (2015).
825
- 826 Sela-Adler, M., Herut, B., Bar-Or, I., Antler, G., Eliani-Russak, E., Levy, E., Makovsky, Y. & Sivan, O.
827 Geochemical evidence for the biogenic methane production and consumption in the shallow sediments of
828 the SE Mediterranean shelf (Israel). *Cont. Shelf Res.* 101, 117-124, (2015).
829



- 830 Silva, High Quality Ribosomal RNA Databases (2016). Available at: <http://www.arb-silva.de> (Accessed 10
831 May 2016).
832
- 833 Sivan, O., Adler, M., Pearson, A., Gelman, F., Bar-Or, I., John, S.G. & Eckhert, W. Geochemical evidence
834 for iron-mediated anaerobic oxidation of methane. *Limnol. Oceanogr.* 56(4), 1536-1544, (2011).
835
- 836 Stoecker, K. et al. Cohn's Crenothrix is a filamentous methane oxidizer with an unusual methane
837 monooxygenase. *PNAS* 103, 2363-2367, (2006).
838
- 839 Stolper, D.A., Sessions, A.L., Ferreira, A.A., Santos Neto, E.V., Schimmelmann, S.S., Valentine, D.L. &
840 Eiler, J.M. Combined ¹³C-D and D-D clumping in methane: Methods and preliminary results. *Geochim. et*
841 *Cosmochim. Acta* 126, 169-191, (2014).
842
- 843 Timmers, P.H.A., Suarez-Zuluaga, D.A., van Rossem, M., Diender, M., Stams, A.J.M. & Plugge, C.M.
844 Anaerobic oxidation of methane associated with sulfate reduction in a natural freshwater gas source. *ISME*
845 *J.* 10, 1400-1412, (2015).
846
- 847 Valentine, D.L. & Reeburgh, W.S. New perspectives on anaerobic methane oxidation. *Environ. Microbiol.*
848 2, 477-484, (2000).
849
- 850 Vengosh, A., Jackson, R.B., Warner, N., Darrah, T.H. & Kondash, A. A Critical Review of the Risks to
851 Water Resources from Unconventional Shale Gas Development and Hydraulic Fracturing in the United
852 States. *Environ. Sci. Technol.* 48, 8334-8348, (2014).
853
- 854 Vetriani, C., Jannash, H.W., MacGregor, B.J., Stahl, D.A. & Reysenbach, A.L. Population structure and
855 phylogenetic characterisation of marine benthic archaea in deep-sea sediments. *Appl. Environ. Microbiol.*
856 65, 4375-4384, (1999).
857
- 858 Vidic, R.D., Brantley, S.L., Vandenbossche, J.M., Yoxtheimer, D. & Abad, J.D. Impact of Shale Gas
859 Development on Regional Water Quality. *Science*. 340, 1235009-1-9, (2013).
860
- 861 Wagner, M., Roger, A.J., Flax, J.L., Brusseau, G.A. & Stahl, D.A. Phylogeny of dissimilatory sulfite
862 reductases supports an early origin of sulfate respiration. *J. Bacteriol.* 180, 2975-2982, (1998).
863
- 864 Wang, D.T. et al. Nonequilibrium clumped isotope signals in microbial methane. *Science* 348 (6233), 428-
865 431, (2015).
866



- 867 Ward, C.R. & Kelly, B.F.J. Background Paper on New South Wales Geology. University of New South
868 Wales, Sydney, Australia, (2007).
869
- 870 Whiticar, M.J. & Faber, E. Methane oxidation in sediment and water column environments – isotope
871 evidence. *Org. Geochem.* 10, 759-768, (1986).
872
- 873 Whiticar, M.J. Carbon and hydrogen isotope systematics of bacterial formation and oxidation of methane.
874 *Chem. Geol.* 161, 291-314, (1999).
875
- 876 Wilkins, D., van Sebille, E., Rintoul, S.R., Lauro, F.M. & Cavicchioli, R. Advection shapes Southern Ocean
877 microbial assemblages independent of distance and environmental effects. *Nat. Commun.* 4, 2457, (2013).
878
- 879 Wilms, R., Sass, H., Koepke, B., Cypionka, H. & Engelen, B. Methane and sulfate profiles within the
880 subsurface of a tidal flat are reflected by the distribution of sulfate-reducing bacteria and methanogenic
881 archaea. *FEMS Microbiol. Ecol.* 59, 611-621, (2007).
882
- 883 Wimmer, B., Hrad, M., Huber-Humer, M., Watzinger, A., Wyhlidal, S. & Reichenauer, T.G. Stable isotope
884 signatures for characterising the biological stability of landfilled municipal solid waste. *Waste Manage.*
885 33(10), 2083-2090, (2013).
886
- 887 Yoshinaga, M.Y., Holler, T., Goldhammer, T., Wegener, G., Pohlman, J.W., Brunner, B., Kuypers,
888 M.M.M., Hinrichs, K.U. & Elvert, M. Carbon isotope equilibration during sulphate-limited anaerobic
889 oxidation of methane. *Nat. Geosci.* 7, 190-194, (2014).
890
- 891 Zhang, L. & Soeder, D.J. Modeling of methane migration in shallow aquifers from shale gas well drilling.
892 *Groundwater* 54(3), 345-353, (2016).
893
- 894 Zhu, J., Wang, Q., Yuan, M., Tan, G-Y.A., Sun, F., Wang, C., Wu, W. & Lee, P-H. Microbiology and
895 potential applications of aerobic methane oxidation coupled to denitrification (AME-D) process: a review.
896 *Water Res.* 90, 203-215, (2016).
897